Properties of Short-Chain Dehydrogenase/Reductase RalR1: Characterization of Purified Enzyme, Its Orientation in the Microsomal Membrane, and Distribution in Human Tissues and Cell Lines†

Olga V. Belyaeva,‡ Anton V. Stetsenko,‡ Peter Nelson,§,|| and Natalia Y. Kedishvili*,‡

Division of Molecular Biology and Biochemistry, School of Biological Sciences, University of Missouri−Kansas City, Kansas City, Missouri 64110, Departments of Urology and Medicine, University of Washington, Seattle, Washington 98195, and Division of Human Biology, Fred Hutchinson Cancer Research Center, Seattle, Washington 98109

Received July 21, 2003; Revised Manuscript Received September 23, 2003

ABSTRACT: Recently, we reported the first biochemical characterization of a novel member of the short-chain dehydrogenase/reductase superfamily, retinal reductase 1 (RalR1) (Kedishvili et al. (2002) *J. Biol. Chem. 277*, 28909−28915). In the present study, we purified the recombinant enzyme from the microsomal membranes of insect Sf9 cells, determined its catalytic efficiency for the reduction of retinal and the oxidation of retinol, established its transmembrane topology, and examined the distribution of RalR1 in human tissues and cell lines. Purified RalR1-His_6 exhibited the apparent K_m values for all-*trans*-retinal and all-*trans*-retinol of 0.12 and 0.6 μM, respectively. The catalytic efficiency (k_{cat}/K_m) for the reduction of all-*trans*-retinal (150 000 min^{-1} mM^{-1}) was 8-fold higher than that for the oxidation of all-*trans*-retinol (18 000 min^{-1} mM^{-1}). Protease protection assays and site-directed mutagenesis suggested that the enzyme is anchored in the membrane by the N-terminal signal-anchor domain, with the majority of the polypeptide chain located on the cytosolic side of the membrane. An important feature that prevented the translocation of RalR1 across the membrane was the positively charged $R^{25}K$ motif flanking the N-terminal signal-anchor. The cytosolic orientation of RalR1 suggested that, in intact cells, the enzyme would function predominantly as a reductase. Western blot analysis revealed that RalR1 is expressed in a wide variety of normal human tissues and cancer cell lines. The expression pattern and the high catalytic efficiency of RalR1 are consistent with the hypothesis that RalR1 contributes to the reduction of retinal in various human tissues.

Short-chain dehydrogenases/reductases (SDR)[1] comprise a large family of functionally heterogeneous proteins that participate in the metabolism of steroids, prostaglandins, retinoids, aliphatic alcohols, and xenobiotics (reviewed in refs *1* and *2*). Members of the SDR superfamily are found in the cytoplasm, mitochondria, nuclei, peroxisomes, and endoplasmic reticulum. Many enzymes that act on the same endogenous substrate exhibit different subcellular localization, cofactor specificity, substrate affinity, tissue distribution, and direction of the reaction (reviewed in ref *3*). In general, those SDR enzymes that prefer NAD^+ as a cofactor function as dehydrogenases in vivo, whereas those that prefer $NADP^+$ function as reductases (*3*). For integral membrane proteins, their transmembrane orientation determines the availability of cofactors, and therefore, the direction of the reaction (*4*−*6*).

To date, about 3000 primary structures from various species have been annotated in sequence databases as members of the SDR superfamily based on SDR signature features such as the TGX_3GXG motif of the nucleotide binding region and the catalytically active tetrad N−S−Y−K, which constitutes the active site (*1*). At least 63 SDR genes have been identified in the human genome database (*1*). For many of these putative oxidoreductases, their cellular functions are yet to be determined. One such enzyme is encoded by a human gene that is expressed at much higher mRNA levels in the human prostate as compared to other tissues, hence the original name prostate short-chain dehydrogenase/reductase (PSDR1) (*7*). Recently, we reported the first biochemical characterization of the protein encoded by the human PSDR1 gene (*8*). PSDR1 was found to be associated with the membranes of the endoplasmic reticulum and recognized all-*trans*- and *cis*-retinoids as substrates (*8*). The membrane-bound enzyme exhibited a preference for $NADP^+$ and NADPH as cofactors and was more efficient in the reductive than in the oxidative direction in vitro. Accordingly, PSDR1 was renamed RalR1 for retinal reductase 1 (*8*). In this study, we purified the recombinant enzyme from Sf9 cells, determined its catalytic efficiency for the reduction of retinal and the oxidation of retinol, established

† Supported by the National Institute on Alcohol Abuse and Alcoholism Grant AA12153 to N.Y.K. and by grants from the National Cancer Institute CA75173 and Department of Defense PC991274 to P.S.N.

* To whom correspondence should be addressed. Phone: (816) 235-2658. Fax: (816) 235-5595. E-mail: kedishvilin@umkc.edu.

‡ University of Missouri−Kansas City.

§ University of Washington.

|| Fred Hutchinson Cancer Research Center.

[1] Abbreviations: SDR, short-chain dehydrogenase/reductase; PSDR1, prostate short-chain dehydrogenase/reductase 1; RalR1, retinaldehyde reductase 1; SDS−PAGE, polyacrylamide gel electrophoresis in the presence of sodium dodecyl sulfate; PMSF, phenylmethylsulfonyl fluoride; Endo H, endoglycosidase H; DHPC, 1,2-diheptanoyl-*sn*-glycero-3-phosphocholine; DTT, dithiothreitol.

10.1021/bi035288u CCC: $25.00
Published on Web 11/22/2003

its orientation in the microsomal membranes, and investigated its expression pattern in human cells and tissues to obtain a better understanding of the properties and the physiological role of RalR1.

EXPERIMENTAL PROCEDURES

Construction of His$_6$-Tagged RalR1 Expression Vector. The coding region of full-length RalR1 cloned into the *Eco*RI restriction site of pCR2.1-TOPO vector was PCR-amplified using the forward primer 5′-GCCACCATGGTTGAGCTCATGTTCCCG-3′, containing an *Nco*I restriction site (underlined), and the reverse primer 5′-TCGCAAGCTTGTCTATTGGGAGGCCCAGCAGG-3′, containing a *Hind*III restriction site (underlined). PCR amplification was performed for 35 cycles, with denaturation for 1 min at 94 °C, annealing for 1 min at 60 °C, and elongation for 2 min at 72 °C. The PCR product was gel-purified using the QIAQuick gel extraction kit (Qiagen Inc., Valencia, CA), digested with *Nco*I and *Hind*III restriction endonucleases, and cloned into the respective sites of pET28a vector (Novagen, Madison, WI) to create an in-frame C-terminal fusion of RalR1 cDNA with a His$_6$-tag in pET28a. To transfer the RalR1-His$_6$ fusion cassette to baculovirus transfer vector pVL1393 (BD Biosciences Pharmingen, San Diego, CA), pET28a vector was first cleaved at the *Dra*III restriction site flanking the RalR1-His$_6$ insert at the 3′ end. The cleavage site was blunt-ended with T4 DNA polymerase (New England Biolabs, Inc., Beverly, MA). The RalR1-His$_6$ insert was excised from the pET28a plasmid at the *Xba*I restriction site flanking the 5′ end of the RalR1 cDNA. The *Xba*I-blunt RalR1-His$_6$ cDNA was gel-purified and cloned into the pVL1393 vector, which was first cleaved with *Pst*I, blunt-ended, and cleaved with *Xba*I to provide a cohesive end for RalR1-His$_6$ cDNA ligation. The final construct was verified by DNA sequencing. Recombinant baculovirus was produced by cotransfection of Sf9 cells with the transfer vector and the linearized Sapphire Baculovirus DNA (Orbigen Inc., San Diego, CA) according to the manufacturer's instructions.

Expression and Purification of Recombinant RalR1-His$_6$. Expression of recombinant RalR1-His$_6$ was carried out as described previously for wild-type RalR1 (*8*). Sf9 cells expressing the RalR1-His$_6$ protein were collected by centrifugation; washed with 100 mM potassium phosphate, 150 mM potassium chloride, 20% (w/v) glycerol, 2 mM β-mercaptoethanol; and resuspended in the same buffer. The cell suspension was homogenized using a French press minicell at 800 psi, and the total homogenate was solubilized by the addition of 1,2-diheptanoyl-*sn*-glycero-3-phosphocholine (DHPC) (Avanti Polar Lipids, Alabaster, AL) as described previously (*9*). A 200 mM stock solution of DHPC in 10 mM potassium phosphate, 20% glycerol, was added to the homogenate dropwise under vortexing to the final concentration of DHPC of 15 mM. The ratio of the total protein to DHPC was 1:1.2 (mg/mg). DHPC-solubilized homogenate was vortexed for 30 min and then centrifuged at 105 000*g* for 1 h at 4 °C (Beckman Optima LE-80K ultracentrifuge, rotor SW 55Ti). The supernatant was supplemented with 5 mM imidazole and loaded onto a Ni^{2+}-NTA metal affinity column (Qiagen Inc.). The resin was washed with 80 column volumes of 10 mM imidazole in 20 mM potassium phosphate, 300 mM sodium chloride, 2 mM DHPC, 20% glycerol, and then with 3 column volumes of 50 mM imidazole in 20 mM potassium phosphate, 150 mM sodium chloride, 1 mM DHPC, 20% glycerol. RalR1-His$_6$ was eluted with a gradient of 100−250 mM imidazole in the above buffer. Fractions were analyzed by electrophoresis in 12% denaturing polyacrylamide gel in the presence of sodium dodecyl sulfate (SDS−PAGE). The fractions that contained homogeneous RalR1 were combined and concentrated. To remove imidazole, the buffer in the eluate was exchanged for 100 mM potassium phosphate, pH 7.4, 40 mM potassium chloride, 1 mM DHPC, 1 mM dithiothreitol (DTT), 20% glycerol, using PD-10 gel-filtration columns (Amersham Biosciences, Piscataway, NJ). Protein concentration was determined as described by Lowry et al. (*10*) using bovine serum albumin as a standard. Purified RalR1-His$_6$ preparations were stored at −80 °C for several months without a loss of activity.

HPLC Analysis of RalR1 Activity. The catalytic activity of RalR1 was assayed in 90 mM potassium phosphate, pH 7.4, and 40 mM KCl at 37 °C (reaction buffer) in siliconized glass tubes as described previously (*8*). Stock solutions of all-*trans*-retinol and all-*trans*-retinal (Sigma-Aldrich, St. Louis, MO) were prepared in ethanol. Ethanol-dissolved retinoids were solubilized in the reaction buffer by a 10 min sonication in the presence of equimolar delipidated bovine serum albumin. Concentrations of ethanol in the reaction mixture did not exceed 1%. The 500 μL reactions were started by the addition of cofactor and carried out for 15 min at 37 °C. Retinaldehyde produced in the oxidative reactions was converted to retinal oximes by the addition of 20 μL of 2 M hydroxylamine (pH 6.3) (*11*). Reaction products were extracted twice with 2 mL of hexane. Hexane was evaporated under nitrogen flow, and retinoids were dissolved in 200 μL of HPLC mobile phase (hexane/acetone, 90:10). Samples were analyzed at 350 nm using a 2487 Dual Absorbance Detector integrated into Waters Alliance HPLC System. The stationary phase was Waters Spherisorb S3W column (4.6 × 100 mm). The flow rate was 1 mL/min. Under these conditions, the elution times were as follows: 2.09 min for all-*trans*-retinaldehyde; 4.095 min for all-*trans*-retinol; and 2.65 min for retinal oxime. Retinoids were quantified by comparing their peak areas to a calibration curve constructed from peak areas of a series of standards.

Determination of Kinetic Constants. The apparent K_m values for the reduction of all-*trans*-retinal were determined at 1 mM NADPH and six concentrations of all-*trans*-retinal (0.05−3.2 μM). The apparent K_m values for the oxidation of all-*trans*-retinol were determined at 1 mM $NADP^+$ and six concentrations of all-*trans*-retinol (0.1−3.2 μM). The apparent K_m values for cofactors were determined at 5 μM all-*trans*-retinal or all-*trans*-retinol and five to six concentrations of one of the following cofactors: NADPH (0.1−6.4 μM), $NADP^+$ (0.2−51.2 μM), NADH (0.2−6.4 mM), or NAD^+ (0.4−6.4 mM). The concentration of purified RalR1-His$_6$ in the reaction mixture varied between 0.02 and 0.1 μg/mL, so that the amount of the product did not exceed 10% of the initial substrate amount. The background value without cofactor was determined for each concentration of substrate and was subtracted from each data point. The experimental values were at least 4-fold higher than the background values. Initial velocities (nmol/min of product formed per mg of protein) were obtained by nonlinear regression analysis. Kinetic constants were calculated using GraFit (Erithacus Software Ltd., UK) and expressed as the

means ± SD. Shown are the results representative of three to four experiments.

Protease Protection Assays. Wild-type or His_6-tagged RalR1 was expressed in Sf9 insect cells using the BaculoGold baculovirus expression system as described previously (*8*). The microsomal fraction was isolated by centrifugation of the post-mitochondrial supernatant at 105 000*g* for 1 h through a 0.6 M sucrose cushion (*12*). Microsomes were resuspended in 100 mM potassium phosphate, pH 7.4, 0.1 mM EDTA, 1 mM DTT, and 20% glycerol.

For protease protection assays, freshly prepared RalR1 microsomes were diluted in 100 mM potassium phosphate, pH 7.4, 40 mM potassium chloride, and 20% glycerol to the final concentration of 1 mg/mL. The suspension was incubated with trypsin (Worthington, Freehold, NJ) or proteinase K (Worthington) for 1 h at 4 or 25 °C in the presence or absence of 1% Triton X-100. The ratio of the protease to the microsomal protein was 1:10 or 1:30 (μg/μg) as indicated. Trypsin digestions were stopped by the addition of an equimolar amount of trypsin inhibitor (Sigma-Aldrich). Proteinase K was inactivated by the addition of phenylmethylsulfonyl fluoride (PMSF) to the final concentration of 4 mM. Digested proteins were analyzed by SDS−PAGE and Western blotting.

Western Blot Analysis. Protein samples were separated in 12% SDS−PAGE and transferred to Hybond-P membrane (Amersham Biosciences). The membrane was blocked with a 5% solution of bovine serum albumin in 20 mM Tris, pH 7.6, 137 mM NaCl, and 0.1% Tween 20 and incubated with different antibodies as indicated. Mouse monoclonal antibodies against the peptide spanning the amino acid residues 287−303 of RalR1 (antibodies #1) were used at a 1:100 dilution. Rabbit polyclonal antibodies raised against a mixture of the N-terminal peptide MVELMFP and the C-terminal peptide LLGLPID of the human RalR1 (antibodies #2) (anti-PSDR1 antibodies, Orbigen Inc.) were used at a 1:2000 dilution. Mouse monoclonal antibodies against His_6-tag (Clontech BD Biosciences, Palo Alto, CA) were used at a 1:3000 dilution. Rabbit anti-human cytochrome P450 reductase polyclonal antibodies (Chemicon International, Inc., Temecula, CA) were used at a 1:5000 dilution. RalR1 protein was detected using an ECL Western blotting analysis system (Amersham Biosciences) as described previously (*8*).

Preparation of RalR1 Tryptic Fragment for Protein Sequencing. A freshly thawed suspension of RalR1-containing microsomes was solubilized using DHPC as described previously. Solubilized microsomal proteins were centrifuged at 105 000*g* for 1 h at 4 °C. The supernatant containing RalR1 was treated with trypsin on ice overnight at a 1:10 trypsin-to-protein ratio (μg/μg). A total of 250 μg of trypsin-treated DHPC extract was separated in SDS−PAGE and transferred to a PVDF membrane. The proteolytic fragment was visualized by Ponceau staining, excised, and subjected to protein sequencing in the Core Laboratories of the Louisiana State University Health Sciences Center in New Orleans (Dr. Jim Carlton).

Site-Directed Mutagenesis of RalR1. Site-directed mutagenesis was carried out on RalR1 cDNA cloned into the *Eco*RI restriction site of pCR2.1-TOPO vector using an ExSite PCR-based kit (Stratagene, La Jolla, CA). R^{25} and K^{26} were substituted for glycine and isoleucine, respectively (construct R25G,K26I), using primers 5′-CCAAATCGGGATAATGCTGAGTG-3′ (substitutions underlined) and 5′-GGCGCAGCCATATACAGAAGGA-3′. The cDNA for R25G,K26I was verified by sequencing and cloned into the *Eco*RI restriction site of pVL1393 baculovirus transfer vector. A pVL1393 vector with the correct orientation of the insert was identified based on the restriction digest. Cotransfection of Sf9 cells with R25G,K26I-pVL1393 and Sapphire baculovirus DNA was carried out according to the manufacturer's protocol (Orbigen Inc.) (*8*).

Coupled in Vitro Transcription/Translation. For in vitro protein synthesis, wild-type and R25G,K26I RalR1 cDNAs cloned into the pCR2.1-TOPO vector were subjected to coupled transcription/translation in the presence or absence of dog pancreas microsomes using TNT Quick system (Promega, Madison, WI) (*8*). In a typical assay, 0.5−1 μg of plasmid DNA, 10 μCi of [^{35}S]-methionine (Amersham Biosciences), and 0.5 μL of microsomal membranes (Promega) were incubated for 90 min at 30 °C in the final volume of 12.5 μL. ^{35}S-Labeled proteins were subjected to 12% SDS−PAGE and analyzed by autoradiography.

Endoglycosidase H (Endo H) Treatment. Twenty micrograms of Sf9 microsomes or 5 μL of an in vitro translated protein sample were diluted in 50 mM sodium phosphate buffer, pH 5.5, containing 0.1% SDS and 0.1 M β-mercaptoethanol to the final volume of 13 μL. Protease inhibitor PMSF was added to the final concentration of 5 mM. One-half of the mixture was treated with 2.5 μL (12.5 units) of Endo H (Roche Applied Science, Indianapolis, IN), and the other half received 2.5 μL of the buffer. Both samples were incubated overnight at room temperature, then denatured with SDS−PAGE loading buffer for 5 min at 94 °C and analyzed by Western blotting or autoradiography.

Analysis of RalR1 Expression in Human Tissues and Cells. Samples of frozen human tissues (Anatomical Gift Foundation, Laurel, MD) were homogenized in 50 mM Hepes, pH 6.8, 2 mM DTT, 1 mM benzamidine, and 1 mM EDTA and centrifuged at 20 000*g* for 30 min, followed by a 2 h centrifugation of the supernatant at 105 000*g* to isolate the light particulate fraction. Microsomal fractions from liver and jejunum were obtained from Tissue Transformation Technologies (Edison, NJ) and the BioChain Institute, Inc. (Hayward, CA).

Human cell lines obtained from American Type Culture Collection (Manassas, VA) were grown in a humidified atmosphere in 5% CO_2 at 37 °C in the presence of 10% fetal bovine serum or heat-inactivated horse serum (HEK-293 cells), 100 units/mL of penicillin, and 100 μg/mL streptomycin. SK−N−SH neuroblastoma cells, HepG2 hepatocytes, and HEK-293 human embryonal kidney cells were cultured in Eagle's Minimal Essential Medium (EMEM). LNCaP prostate cancer cells were cultured in RPMI-1640 media. SH−SY5Y neuroblastoma cells were cultured in a 1:1 mixture of F12 medium and EMEM with nonessential amino acids.

To isolate the microsomal fractions, cultured cells were homogenized using a French Press mini-cell at 800 psi. The homogenate was centrifuged at 3000*g* for 15 min to remove the unbroken cells and nuclei. The 3000*g* supernatant was centrifuged at 10 000*g* for 30 min to remove the mitochondria. Microsomes were isolated by centrifugation of the post-mitochondrial supernatant at 105 000*g* for 60 min through a cushion of 0.6 M sucrose (*12*).

```
1    MVELMFPLLL LLLPFLLYMA APQIRKMLSS GVCTSTVQLP GKVVVVTGAN   50
51   TGIGKETAKE LAQRGARVYL ACRDVEKGEL VAKEIQTTTG NQQVLVRKLD  100
101  LSDTKSIRAF AKGFLAEEKH LHVLINNAGV MMCPYSKTAD GFEMHIGVNH  150
151  LGHFLLTHLL LEKLKESAPS RIVNVSSLAH HLGRIHFHNL QGEKFYNAGL  200
201  AYCHSKLANI LFTQELARRL KGSGVTTYSV HPGTVQSELV RHSSFMRWMW  250
251  WLFSFFIKTP QQGAQTSLHC ALTEGLEILS GNHFSDCHVA WVSVQARNET  300
301  IARRLWDVSC DLLGLPIDKL AAALEHHHHH H
```

FIGURE 1: RalR1 primary structure. The N-terminal hydrophobic segment comprised of the first 2−22 amino acid residues is highlighted in gray. The positively charged motif $R^{25}K$ following the hydrophobic segment is shown in bold. The trypsin cleavage sites are indicated by arrows. The endogenous glycosylation consensus motifs are shown in bold italic. The peptide recognized by antibodies #1 is doubly underlined. The peptides recognized by antibodies #2 are indicated by dashed lines. The last amino acid residue of RalR1 is indicated by a star. The amino acid residues added to RalR1 polypeptide in RalR1-His_6 fusion protein are italicized.

Table 1: Purification of Recombinant RalR1-His_6 from Sf9 Cells[a]

purification step	specific activity, nmol/min mg	activity yield, %	total protein, mg	protein recovery, %	purification (*n*-fold)
homogenate	44	100	72	100	1.0
DHPC extract	56	95	54	75	1.3
eluate	630	35	1.7	2.4	14

[a] The results shown are representative of three independent preparations. The specific activity of RalR1 at different stages of purification was determined with 5 μM all-*trans*-retinal and 1 mM NADPH.

Membrane proteins from human cells and tissues were separated by 12% SDS−PAGE and transferred to Hybond-P membrane. Expression of RalR1 was analyzed using antibodies #2 as described under the section *Western Blot Analysis*.

RESULTS

Purification and Kinetic Characterization of Recombinant RalR1-His_6. Previous analysis of the substrate and cofactor specificity of RalR1 was carried out using microsomal preparations of the enzyme (*8*). Membrane-associated components could impact the activity and kinetics of RalR1. To determine the kinetic parameters of RalR1 under well-defined conditions, we prepared a new baculovirus expression construct coding for a C-terminal fusion of RalR1 to a His_6-tag (Figure 1) to purify RalR1 in one step using affinity chromatography (Experimental Procedures). The N-terminus of RalR1 was left intact to ensure proper targeting of the recombinant protein to the microsomal membranes. The expression level of RalR1-His_6 in Sf9 cells was similar to that of the wild-type protein. RalR1-His_6 was associated with the microsomal membranes and exhibited a retinal reductase activity comparable to that of wild-type RalR1.

To extract and purify the His_6-tagged protein from the microsomal membranes, Sf9 cells were collected by centrifugation and homogenized, and the membrane-bound proteins were solubilized with a mild lipid-like detergent DHPC (Experimental Procedures). Fifteen millimolar DHPC solubilized 95% of the recombinant protein according to the activity measurements (Table 1) and Western blot analysis of the 105 000*g* pellet and supernatant obtained after centrifugation of the detergent-extracted homogenate (data not shown). Solubilized RalR1-His_6 was purified to homogeneity in a single step using Ni^{2+}-affinity chromatography (Figure 2). Most contaminants were removed by washing the column with 10−50 mM imidazole. The wash fractions

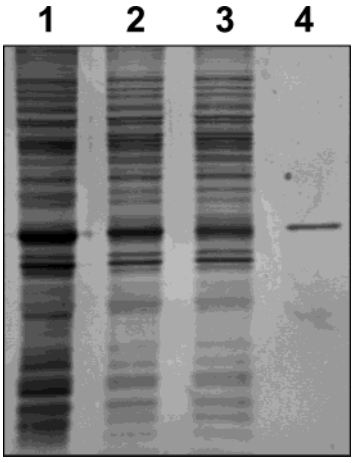

FIGURE 2: Purification of RalR1-His_6 fusion protein. Samples of RalR1-His_6-containing fractions were analyzed by SDS−PAGE. Proteins were visualized by silver staining. Lane 1, homogenate of RalR1-His_6-expressing Sf9 cells (6 μg); lane 2, DHPC extract (3 μg); lane 3, flow through the Ni^{2+}-NTA metal affinity column (3 μg); and lane 4, purified RalR1-His_6 fusion protein (0.14 μg).

and the pass-through contained approximately 30% of the total RalR1 activity. The more tightly bound RalR1-His_6 was eluted with a gradient of 100−250 mM imidazole. The concentration of DHPC in the elution buffer was decreased to 1 mM. RalR1-His_6 remained soluble at the lower concentration of the detergent. Fractions of the eluate that contained a single protein band of ~36 kDa, recognized by anti-RalR1 antibodies (data not shown), were combined and concentrated (Figure 2, lane 4). The final preparation of RalR1-His_6 was more than 90% pure as judged by SDS−PAGE and densitometric analysis. The typical yield was ~1.7 mg of homogeneous enzyme with a specific activity of 500−630 nmol/min mg from ~5×10^8 of Sf9 cells (Table 1). Purified RalR1-His_6 was stored at −80 °C in a buffer containing 1 mM DHPC. The frozen enzyme was catalytically stable for several months. At 8 °C in a refrigerator, the enzyme retained nearly full activity for at least one month. For activity assays, the purified enzyme was diluted 100-fold with a detergent-free reaction buffer. This reduced the concentration of DHPC in the enzyme preparation from 1 to 0.01 mM. The diluted enzyme remained soluble and active when stored frozen in small aliquots at −80 °C. The addition of DHPC to 15 mM did not increase the activity of the diluted enzyme.

Purified His_6-tagged RalR1, which contained a C-terminal extension of 13 amino acids, exhibited kinetic parameters

Table 2: Kinetic Constants of the Membrane-Bound Wild-Type RalR1 and Purified RalR1-His_6[a]

substrate/cofactor	apparent K_m, μM		apparent V_{max}, nmol/min mg	
	membrane-bound wild-type RalR1	purified RalR1-His_6	membrane-bound wild-type RalR1	purified RalR1-His_6
all-*trans*-retinal determined with NADPH	0.20 ± 0.01	0.12 ± 0.1	41 ± 1	506 ± 13
all-*trans*-retinol determined with $NADP^+$	0.70 ± 0.04	0.6 ± 0.1	13.2 ± 0.3	300 ± 20
$NADP^+$	0.4 ± 0.2	1.0 ± 0.1	8.7 ± 0.8	250 ± 4
NAD^+	680[b]	2500 ± 190		150 ± 5
NADPH	0.48 ± 0.02	0.47 ± 0.04	44.0 ± 0.6	530 ± 10
NADH	1300[b]	1300 ± 120		910 ± 30

[a] Kinetic constants for the reduction of all-*trans*-retinal were determined in the presence of saturating NADPH (1 mM) (Experimental Procedures). Kinetic constants for the oxidation of all-*trans*-retinol were determined at saturating $NADP^+$ (1 mM). The apparent K_m values for cofactors were determined at fixed concentrations of all-*trans*-retinal and all-*trans*-retinol (5 μM each). [b] Reported in ref *8*.

similar to those of the membrane-bound wild-type enzyme. The apparent K_m values of purified RalR1-His_6 for all-*trans*-retinal and all-*trans*-retinol were 0.12 and 0.6 μM, respectively, as compared to the corresponding values of 0.2 and 0.7 μM for wild-type membrane-bound RalR1 (Table 2). Purified RalR1-His_6 exhibited a preference for $NADP^+$ and NADPH with the apparent K_m values of 1 and 0.47 μM versus 680 and 2500 μM for NAD^+ and NADH (Table 2). Like the membrane-bound wild-type enzyme, purified RalR1-His_6 exhibited a higher rate of retinal reduction as compared to retinol oxidation (Table 2). From the V_{max} value of 506 nmol/min mg for retinal reduction and the subunit molecular mass of ~35.4 kDa, we calculated that the k_{cat} value of RalR1-His_6 in the reductive direction with all-*trans*-retinal as substrate and NADPH as cofactor was 18 min^{-1}, translating into the catalytic efficiency (k_{cat}/K_m) of 150 000 min^{-1} mM^{-1}. The k_{cat} value and the catalytic efficiency in the oxidative direction using all-*trans*-retinol as substrate and $NADP^+$ as cofactor were 11 min^{-1} and 18 000 min^{-1} mM^{-1}, respectively. Thus, RalR1-His_6 exhibited kinetic constants very similar to those of the wild-type enzyme and was ~8-fold more catalytically efficient as a retinal reductase than as a retinol dehydrogenase.

Orientation of RalR1 in the Membrane. Previously, we established that RalR1 is an integral membrane protein associated with the microsomal membranes (*8*). To determine whether RalR1 utilizes the lumenal or the cytosolic pool of nicotinamide adenine dinucleotide cofactors, we investigated the transmembrane orientation of RalR1 using a number of different approaches. First, the microsomal vesicles containing recombinant RalR1 were incubated with proteinase K or trypsin in the presence of 1% Triton X-100 (permeabilized vesicles) or in the absence of detergent (sealed vesicles). It was expected that the segments of RalR1 facing the cytosolic side of the membrane would be digested by proteases, whereas the segments located in the lumen would be protected by the membrane in sealed vesicles and digested in Triton-permeabilized vesicles.

The membrane-bound recombinant RalR1 was resistant to proteolysis at 4 °C with or without Triton X-100 (data not shown). At room temperature, treatment of sealed RalR1-microsomes with trypsin in the absence of detergent produced a single RalR1 fragment that was only slightly shorter (~33 kDa) than the full-length RalR1 (~35 kDa) (Figure 3A). This fragment was recognized by RalR1-specific antibodies (data not shown) and was resistant to further proteolysis. A similar proteolytic pattern was observed with a microsomal preparation of native human RalR1 treated with proteinase K (Figure 3B). In contrast, microsomal cytochrome P450 reductase (*13*) was fully digested under these conditions (Figure 3B).

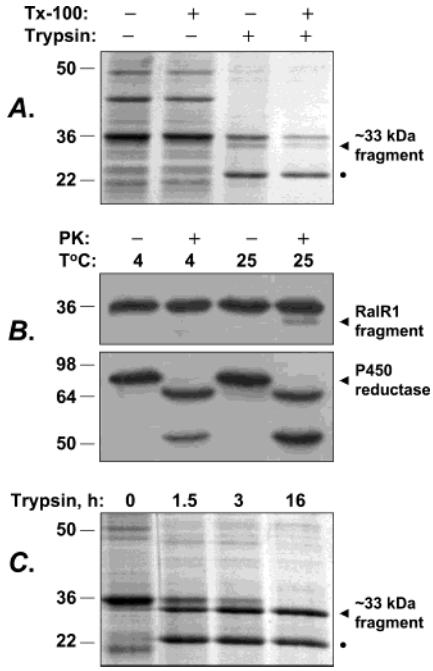

FIGURE 3: Protease protection assays. (A) RalR1-containing Sf9 microsomes (10 μg) were treated with trypsin (1 μg) in the presence (+) or absence (−) of 1% Triton X-100 (Tx-100) for 1 h at 25 °C. Proteins were separated in SDS−PAGE and visualized by staining with Coomassie Brilliant Blue R-250. RalR1 proteolytic fragment is indicated by an arrow. Dot indicates the position of added trypsin. (B) Female liver microsomes were treated with Proteinase K (PK) at a 30:1 ratio (μg/μg) for 2 h at 4 or 25 °C. RalR1 and cytochrome P450 reductase were detected by Western blot analysis as described under Experimental Procedures. (C) DHPC extract of RalR1-containing microsomes was treated with trypsin on ice (Experimental Procedures). Twenty-five microgram aliquots of the digestion mixture were withdrawn at indicated times and analyzed by SDS−PAGE as described under panel A.

The addition of a detergent to the membranes did not change the overall proteolytic pattern of RalR1 (Figure 3A) but appeared to facilitate the formation of a ~33 kDa fragment (Figure 3C). Incubation of RalR1-containing microsomes with trypsin in the presence of DHPC resulted in the appearance of ~33 kDa fragment after only 1.5 h of incubation on ice (Figure 3C). After 16 h, RalR1 was fully converted into the ~33 kDa fragment (Figure 3C). This RalR1 fragment was not only remarkably stable and resistant to proteolysis but also retained ~95% of catalytic activity.

To determine whether the cleavage occurred on the N- or the C-terminal end of RalR1, the ~33 kDa fragment was

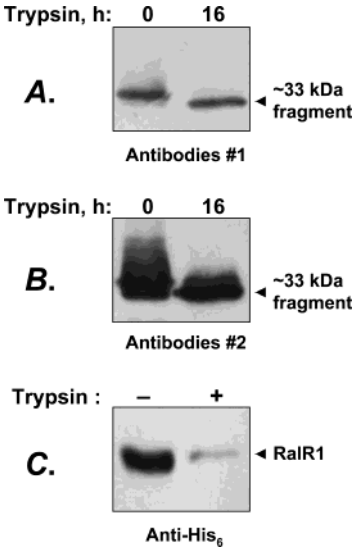

FIGURE 4: Western blot analysis of the C-terminal end of RalR1 fragment. (A and B) DHPC extract of wild-type RalR1 microsomes (25 μg) was treated with trypsin as described in the legend to Figure 2B and under Experimental Procedures. The resulting products were tested for reactivity with antibodies against RalR1 amino acid residues 287−303 (A, antibodies #1) and 1−7 plus 313−318 (B, antibodies #2). (C) Microsomal preparation of histidine-tagged RalR1 (9 μg) was treated with trypsin at 25 °C for 1 h in the absence of detergent and immunostained with anti-His_6-tag antibodies (anti-His_6) used at a 1:3000 dilution. Position of full-length RalR1 is indicated by an arrow.

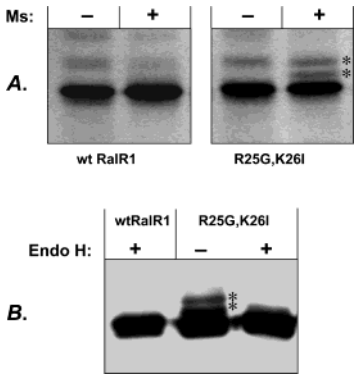

FIGURE 5: Analysis of R25G,K26I Glycosylation. (A) ^{35}S-Labeled wild-type RalR1 and R25G,K26I were synthesized in vitro in the presence (+) or in the absence (−) of canine microsomes using coupled transcription/translation system. Two and a half microliters of the reaction mixture were separated in SDS−PAGE, and the proteins were visualized by autoradiography. N-Glycosylated protein bands are indicated with asterisks (*). (B) Wild-type and R25G,K26I RalR1-containing Sf9 microsomes were treated with Endo H (+) or incubated with the same volume of buffer (−). Two micrograms of each sample were analyzed by Western blotting as described under Experimental Procedures.

subjected to protein sequencing. The N-terminal sequence of the fragment was determined as KMLSSGVCTST, exactly matching the amino acid residues K^{26} through T^{36} of RalR1 polypeptide (Figure 1). This result indicated that the site of trypsin cleavage was on the N-terminal end of RalR1 between residues R^{25} and K^{26} (Figure 1), in agreement with the trypsin recognition sequence.

The 318-amino acid RalR1 polypeptide contains other potential trypsin cleavage sites, some of which are located very close to the C-terminus (R^{303} and R^{304}) (Figure 1). Loss of the most C-terminal residues during trypsin digestion might not have been detected by SDS−PAGE analysis. We determined whether the C-terminus was accessible to trypsin by testing the immunoreactivity of the RalR1 fragment with antibodies against the C-terminal peptides. The first antibodies (antibodies #1) recognized the 17-amino acid segment corresponding to residues 287−303 of the RalR1 polypeptide (Experimental Procedures) (Figure 1). The second antibodies (antibodies #2) recognized two segments corresponding to residues 1−7 and 313−318 of RalR1 (Experimental Procedures) (Figure 1). Both preparations of antibodies were able to bind the RalR1 fragment (Figure 4A,B). Since protein sequencing showed that this fragment lacked amino acid residues 1−25, antibodies #2 could bind only to residues 313−318, indicating that the C-terminus of RalR1 fragment was intact. These results suggested that trypsin cleaves the membrane-bound RalR1 only between R^{25} and K^{26}, producing two fragments corresponding to amino acid residues 1−25 and 26−318 of the full-length protein (Figure 1).

To examine the orientation of the C-terminal end of RalR1 in the membrane, we used the His_6-tagged RalR1 expressed in Sf9 cells. RalR1-His_6 was constructed to contain a trypsin cleavage site (K^{320} in Figure 1) between the last amino acid residue of RalR1 (D^{318}) and the attached C-terminal His_6-tag (Figure 1). To determine the orientation of the His_6-tag, freshly isolated microsomes containing RalR1-His_6 were treated with trypsin in the absence or presence of detergent, and the resulting products were analyzed by Western blotting using antibodies against the histidine tag. As shown in Figure 4C, in trypsin-treated membranes in the absence of detergent, there was a significant decrease in the intensity of antibody staining. A similar pattern was observed in the presence of detergent (data not shown). This result indicated that the His_6-tag attached to the C-terminal end of RalR1 was exposed at the cytosolic surface of the membrane.

Role of the Positively Charged N-Terminal Residues in RalR1 Transmembrane Orientation. Algorithms for secondary structure predictions (*14*, *15*) suggest that the N-terminus of RalR1 contains a highly hydrophobic segment of 21 amino acid residues that could serve as a membrane-spanning domain (residues 2−22 in Figure 1). The N-terminal hydrophobic segment is flanked on the C-terminal side by positively charged R^{25} and K^{26} (Figure 1). It is generally believed that the positively charged amino acids immediately downstream of the first hydrophobic domain prevent translocation of the polypeptide chain across the ER membrane (*16*). To explore the role of the $R^{25}K$ motif in the transmembrane orientation of RalR1, we substituted R^{25} and K^{26} for neutral glycine and isoleucine, respectively (R25G,K26I), by site-directed mutagenesis. To determine the transmembrane orientation of R25G,K26I versus wild-type RalR1, both cDNAs were expressed in vitro using a coupled transcription/translation system in the absence or presence of canine pancreatic microsomes. The transmembrane orientation of RalR1 polypeptide in the microsomal membranes was determined based on the glycosylation status of the two endogenous N-glycosylation consensus motifs $N^{174}VS$ and $N^{298}ET$ present in the RalR1 primary structure (Figure 1).

Wild-type RalR1 was not glycosylated and appeared as a single protein band in SDS−PAGE either in the presence or in the absence of microsomes (Figure 5A). On the other hand, R25G,K26I translated in vitro in the presence of microsomes contained two additional slower moving protein

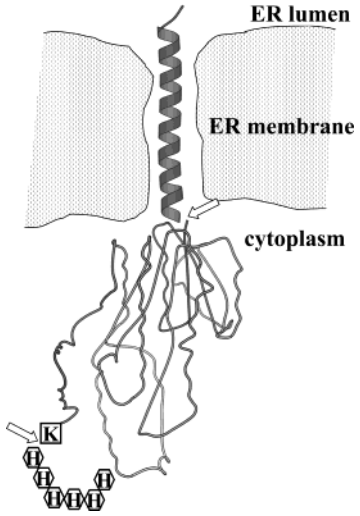

FIGURE 6: Model of RalR1 insertion into the membrane. The sites of trypsin cleavage are indicated by arrows.

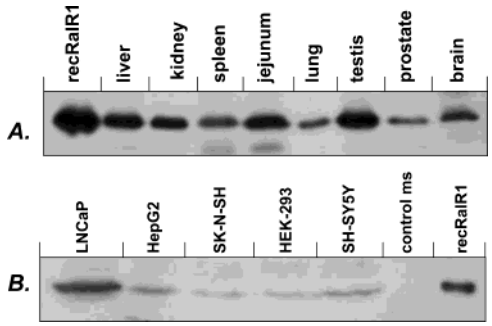

FIGURE 7: Western blot analysis of RalR1 expression in human tissues and cells. (A) Membrane-bound proteins isolated from human liver (44 μg), kidney (22 μg), spleen (71 μg), jejunum (56 μg), lung (36 μg), testis (38 μg), prostate (21 μg), and brain (caudate nucleus, 58 μg). (B) Human cultured cells (100 μg each) were separated by SDS−PAGE and transferred to a PVDF membrane. Western blot analysis was carried out as described under Experimental Procedures. recRalR1, microsomal preparation of recombinant RalR1 expressed in Sf9 cells (0.3 μg in panel A and 0.03 μg in panel B). Control ms, Sf9 microsomes (18 μg).

bands (Figure 5A), which were removed by Endo H treatment (data not shown). Since glycosylation occurs exclusively in the ER lumen, these results suggested that elimination of the positively charged residues at the N-terminus of RalR1 resulted in the inversion of the topology and translocation of the polypeptide chain across the membrane. Coordinated glycosylation of both N^{174} and N^{298} indicated that the two sites are located on the same side of the membrane.

To test whether R25G,K26I assumed an inverted orientation in intact cells, we expressed the corresponding construct in Sf9 cells. As compared to wild-type RalR1 microsomes, R25G,K26I microsomes contained two additional protein bands that were recognized by RalR1 antibodies (Figure 5B). These two bands were removed by Endo H treatment (Figure 5B), indicating that, similar to the in vitro system, R25G,K26I was glycosylated in intact cells. Thus, both the in vitro and the in vivo experiments suggested that the $R^{25}K$ motif serves as a stop-transfer signal during RalR1 insertion into the membrane.

Taken together, the results of the protease protection assays, Western blot analyses, and site-directed mutagenesis indicated that RalR1 is anchored in the membrane by a single N-terminal domain with the rest of the polypeptide chain facing the cytosolic side of the membrane. A model summarizing these observations is shown in Figure 6.

Expression of RalR1 in Human Tissues and Cultured Cells. Previous examination of RalR1 expression in human tissues by Northern blot analysis suggested that RalR1 mRNA is expressed at a much higher level in human prostate as compared to all other tissues (*7*). To determine whether the RalR1 protein is present in tissues other than prostate, we carried out a Western blot analysis of RalR1 in the light membrane fractions isolated from 10 human organs. Surprisingly, a protein band identical in size to the recombinant RalR1 (recRalR1) was recognized by anti-RalR1 antibodies in eight different tissues (Figure 7A). After normalization of the signal per protein amount by scanning densitometry, the highest level of RalR1 protein was detected in the kidney, followed by testis, liver, jejunum, prostate, lung, brain (caudate nucleus), and spleen. The estimates are approximate since the membranes were isolated from frozen tissue samples and could have been contaminated by membranes from other organelles. RalR1 was not detected in skeletal muscle (19 μg) or heart (30 μg), possibly due to insufficient sensitivity of the antibodies.

In agreement with the previous report (*8*), RalR1 protein was abundant in cultured LNCaP prostate cancer cells (Figure 7B). Lower levels of RalR1 were detected in the same amount of microsomes from HepG2 hepatocytes, HEK-293 embryonal kidney cells, and two neuroblastoma cells lines, SK−N−SH and SH−SY5Y (Figure 7B). Thus, Western blot analysis showed that RalR1 is expressed in a wide variety of normal human tissues and is present at detectable levels in various cancer cells.

DISCUSSION

RalR1 is a novel member of the SDR superfamily that was initially identified at the gene level as a transcript highly expressed in the human prostate (*7*). The protein product of the RalR1 gene was found to be an integral membrane protein (*8*). Since purification of integral membrane proteins is frequently associated with a loss of enzymatic activity, an initial analysis of RalR1 substrate and cofactor specificity was carried out using microsomal preparations of the recombinant enzyme expressed in insect Sf9 cells (*8*). To continue the characterization of RalR1 properties and its structure−function relationships, we purified the enzyme to homogeneity in the present study. Our previous attempts to overexpress RalR1-His_6 fusion protein in *E. coli* as a full-length protein or as a truncated variant lacking the first 26 hydrophobic amino acids were not successful. The bacterially expressed proteins were inactive, and their expression levels in *E. coli* were extremely low (Belyaeva et al., unpublished observations). Therefore, we chose to produce recombinant His_6-tagged RalR1 in insect cells. Like the wild-type protein, His_6-tagged RalR1 was targeted to the microsomal membranes. Importantly, the enzyme was catalytically active and expressed at a relatively high level (~7% of the total cellular protein). His_6-tagged RalR1 was extracted from the membranes without an apparent loss of activity and was purified in a single step using Ni^{2+}-affinity chromatography. Even though a fraction of the recombinant protein bound weakly

to the nickel-chelated affinity matrix, the overall yield of a purified highly active and stable enzyme was in the range of milligrams.

The specific activity of the purified enzyme with all-*trans*-retinal as substrate was 12−14-fold higher than that of the microsomal preparations of wild-type RalR1. Kinetic characterization of purified His_6-tagged RalR1 showed that it exhibits the apparent K_m values for retinoid substrates and nicotinamide dinucleotide cofactors nearly identical to those of the membrane-bound wild-type enzyme. Similar to wild-type membrane-bound RalR1, purified RalR1-His_6 was more catalytically efficient in the reductive direction than in the oxidative. These observations suggested that the 13-amino acid C-terminal extension added to RalR1 did not have a significant impact on the kinetic parameters of the enzyme. Interestingly, although NADH was not the preferred cofactor (K_m value of 1300 μM versus 0.47 μM for NADPH), the V_{max} value with NADH was 1.7-fold higher than that with NADPH. Thus, if the activity of RalR1 was assayed in tissue samples at high millimolar concentrations of cofactors, NADH would appear to be the preferred cofactor.

The actual concentrations of cofactors available to RalR1 in the cells would depend on the transmembrane orientation of the enzyme in the ER membrane. For example, 11β-hydroxysteroid dehydrogenase type I is a membrane-bound glycosylated protein, which is located in the lumen of the endoplasmic reticulum (ER) and functions in the reductive direction in the cells, converting 11-keto- into 11β-hydroxy-glucocorticoids (*4*, *17*). In contrast, 11β-hydroxysteroid dehydrogenase type II, which is also an integral membrane protein, faces the cytosolic side of the ER membrane and catalyzes exclusively the dehydrogenation of 11β-hydroxy-steroids (*4*, *18*). The cisternae of microsomes have been reported to contain 240 μM NAD^+ and 55 μM $NADP^+$ (*19*), and the concentration of free NAD^+ in the cytosol has been determined to be 6 mM (*20*). Although there is little direct information on the concentrations of NADH and NADPH, there is a general agreement that most of the cytosolic nonphosphorylated cofactors exist in the oxidized form, whereas most of the phosphorylated cofactors are reduced, with the ratio of NAD^+/NADH close to ∼1000 and the ratio of $NADP^+$/NADPH close to 0.01 (*21*).

The results of the present study suggest that RalR1 is a type III integral membrane protein that lacks a cleavable ER signal sequence and is anchored in the membrane by the N-terminal hydrophobic signal-anchor domain (Figure 6). The N-terminal signal-anchor followed by the positively charged $R^{25}K$ motif appears to also function as a stop-transfer sequence, preventing further extrusion of the nascent chain into the ER lumen. Substitution of R^{25} and K^{26} for glycine and isoleucine, respectively, allows RalR1 to flip its orientation in the membrane and become glycosylated at the endogenous glycosylation consensus motifs. The polypeptide chain on the cytosolic side of the membrane appears to be folded into a protease-resistant conformation and is connected to the transmembrane domain by a short segment that is more accessible to proteases than the rest of the polypeptide chain.

According to the algorithms for topology predictions (*14*, *15*), RalR1 contains a second hydrophobic segment between residues 228 and 248, which could potentially serve as a transmembrane domain. However, this transmembrane domain would separate the two endogenous glycosylation consensus motifs in the primary structure of RalR1. Our data indicate that N^{174} and N^{298} are glycosylated simultaneously. This observation suggests that the two glycosylation motifs are located on the same side of the membrane, arguing against the existence of the second transmembrane domain. We conclude that the catalytic site of RalR1 faces the cytosol and utilizes the cytosolic pool of nucleotide cofactors. Considering that RalR1 exhibits ∼2500-fold lower K_m values for phosphorylated cofactors, of which NADPH is ∼100-fold more abundant in the cytosol than $NADP^+$, RalR1 is most likely to function in the cells as a retinal reductase.

Previously, we suggested that RalR1 could contribute to the reduction of retinal in the human prostate (*8*). Western blot analysis carried out in the present study revealed that RalR1 is expressed at significant levels in many other human tissues besides prostate and that the mRNA levels of RalR1 do not appear to reflect the levels of the corresponding protein. The wide tissue distribution of RalR1 and its high catalytic efficiency for the reduction of retinal are consistent with the proposed role of RalR1 in retinoid metabolism.

REFERENCES

1. Oppermann, U., Filling, C., Hult, M., Shafqat, N., Wu, X., Lindh, M., Shafqat, J., Nordling, E., Kallberg, Y., Persson, B., and Jörnvall, H. (2003) *Chem. Biol. Interact. 143*−*144*, 247−253.
2. Jörnvall, H., Persson, B., Krook, M., Atrian, S., Gonzalez-Duarte, R., Jeffery, J., and Ghosh, D. (1995) *Biochemistry 34*, 6003−6013.
3. Labrie, F., Luu-The, V., Lin, S. X., Labrie, C., Simard, J., Breton, R., and Belanger, A. (1997) *Steroids 62*, 148−158.
4. Odermatt, A., Arnold, P., Stauffer, A., Frey, B. M., and Frey, F. J. (1999) *J. Biol. Chem. 274*, 28762−28770.
5. Tryggvason, K., Romert, A., and Eriksson, U. (2001) *J. Biol. Chem. 276*, 19253−19258.
6. Simon, A., Romert, A., Gustafson, A. L., McCaffery, J. M., and Eriksson, U. (1999) *J. Cell Sci. 112*, 549−558.
7. Lin, B., White, J. T., Ferguson, C., Wang, S., Vessella, R., Bumgarner, R., True, L. D., Hood, L., and Nelson, P. S. (2001) *Cancer Res. 61*, 1611−1618.
8. Kedishvili, N. Y., Chumakova, O. V., Chetyrkin, S. V., Belyaeva, O. V., Lapshina, E. A., Lin, D. W., Matsumura, M., and Nelson, P. S. (2002) *J. Biol. Chem. 277*, 28909−28915.
9. Lapshina, E. A., Belyaeva, O. V., Chumakova, O. V., and Kedishvili, N. Y. (2003) *Biochemistry 42*, 776−784.
10. Lowry, O. H., Rosebrough, N. H., Farr, A. L., and Randall, R. J. (1951) *J. Biol. Chem. 193*, 265−275.
11. Landers, G. M. (1990) *Methods Enzymol. 189*, 70−80.
12. Graham, J. M. (1998) in *Protein Protocols on CD-ROM* (Walker, J. M., Ed.) *Section 6.5*, Humana Press Inc., Totowa, NJ.
13. Kida, Y., Ohgiya, S., Mihara, K., and Sakaguchi, M. (1998) *Arch. Biochem. Biophys. 351*, 175−179.
14. von Heijne, G. (1992) *J. Mol. Biol. 225*, 487−494.
15. Claros, M. G., and von Heijne, G. (1994) *CABIOS 10*, 685−686.
16. Gafvelin, G., Sakaguchi, M., Andersson, H., and von Heijne, G. (1997) *J. Biol. Chem. 272*, 6119−6127.
17. White, P. C., Mune, T., and Agarwal, A. K. (1997) *Endocr. Rev. 18*, 135−156.
18. Stewart, P. M., and Krozowski, Z. S. (1999) *Vitam. Horm. 57*, 249−324.
19. Bublitz, C., and Lawler, C. A. (1987) *Biochem. J. 245*, 263−267.
20. Devin, A., Nogueira, V., Leverve, X., Guerin, B., and Rigoulet, M. (2001) *Eur. J. Biochem. 268*, 3943−3949.
21. Veech, R. L., Eggleston, L. V., and Krebs, H. A. (1969) *Biochem. J. 115*, 609−619.

BI035288U